Fitness Function Evaluation for Image Reconstruction using Binary Genetic Algorithm for Parallel Ray Transmission Tomography

Shahzad Ahmad Qureshi[1], Sikander M. Mirza[2], M. Arif[3],

[1]Department of Computer & Information Sciences
[2]Department of Physics and Applied Mathematics
[3]Department of Electrical Engineering
Pakistan Institute of Engineering & Applied Sciences (PIEAS), P.O. Nilore, Islamabad 45650, Pakistan.

Summary
Various fitness functions have been evaluated for image reconstruction using Binary Genetic Algorithm (BGA) based parallel ray transmission tomography. The population initialization is carried out using the Filtered Back-Projection (FBP) technique. Various fitness functions used for image reconstruction include: Root Mean Squared error (RMSE), Mean Squared error (MSE), Mean Absolute error (MAE), Relative Squared error (RSE), Root Relative Squared error (RRSE) and Relative Absolute error (RAE). RMSE and MAE outperformed for small as well as large size images with different shape complexities. Mixed selection scheme with two variations of crossover operators, namely Image-Row and Block crossover operators have been used for crossover. Binary mutation operator has been used for creating diversity in local search scope. For 64 × 64 head and lung phantoms, BGA has resulted in PSNR values with RMSE 19.26 and 16.49 respectively and 27.20 and 29.65 dB with MAE.

Key words:
Genetic algorithm, Inverse Radon transform, Filtered Back-Projection, Fitness function.

1. Introduction

Image reconstruction using projections through stochastic tomography techniques for discrete-Inverse Radon Transform (d-IRT) estimation is considered of great importance especially for medical imaging applications. Mathematically, it requires an infinite number of projections to find the exact IRT. The problem is ill-posed and requires techniques that carry out the reverse process of ray-sums or Radon transform. Here, the importance of stochastic processes may be ascribed to the use of lower number of projections and / or in the presence of noise contaminated data. Various medical imaging techniques based on stochastic process, including SPECT and PET, have been investigated in past [1].

Many researchers worked towards the estimation of d-IRT by using stochastic techniques. Luo and Yagle used stochastic tomography for image reconstruction by developing a Kalman filter based approach [2]. Their proposed technique was claimed to have distinct advantage over FPB based reconstructions for simple cases. For complex shapes, including head phantom, both the approaches produced similar results. Therefore, the use of Kalman filter based approach appears to be limited to the situations involving lower number of harmonics only.

Metroplis et al. used the principle of thermodynamic equilibrium in numerical computation for global optimization [3]. The slow cooling aligns atoms in perfect order and forms a single crystal. The phenomenon by which the atoms loose mobility is termed as simulated annealing (SA) [4, 5] . Recently, Qureshi et al. introduced a hybrid Simulated Annealing (HSA) which has been found effective for parallel-ray tomographic image reconstruction. The candidate solution is randomly evolved and the error minimization is achieved by tuning various SA parameters [6].

The stochastic technique of Genetic Algorithm (GA), originally developed by Holland, was based on Darwinian theory of biological evolution [7, 8]. Franconi and Jennison proposed a hybrid algorithm for finding the maximum a posteriori (MAP) estimation of a binary image in Baysian image analysis. They used crossover to merge subsections developed by SA. The partitioning strategy and the use of various deterministic techniques, and the way they may be applied to combine solutions, in place of SA still need to be explored [9].

Li et al. introduced a multi-objective genetic local search algorithm for projections-based image reconstruction. However, results remain dependent on the subjective choice of weight-parameters [10]. Günel and Kent used projections data with a GA based algorithm for the determination of object parameters, including dimensions and attenuation coefficients, with improved signal to noise ratios [11]. Most recently, Qureshi et al. have introduced HCGA technique for the solution of image reconstruction problem. They have used continuous GAs hybridized with inverse Fourier transform for population initialization

Manuscript received January 5, 2007.
Manuscript revised January 25, 2007.

which has been found more effective in comparison to FBP and SA [12].

In this work, the image reconstruction has been carried out using Binary Genetic algorithm (BGA) for various sizes and shape complexities. This work critically evaluates fitness functions using BGA for both binary head and lung phantoms [13]. Various fitness functions that have been evaluated include Root-Mean-Squared error (RMSE) and Mean-Squared error (MSE).

2. Mathematical Model

For BGA, templates are created by using FBP technique in which a low-pass-filter is employed in frequency domain for convolution with the image intensities. In transmission tomography, the transmitted intensities for a particular view angle define the projection for that angle. The coordinate system for the model is shown in Fig. 1. For an object *f(x,y)*, a projection along *(θ, t)–line* is called the Radon transform $P_\theta(t)$ of the object for θ given by [14]:

$$P_\theta(t) = \int_{-\infty}^{\infty}\int_{-\infty}^{\infty} f(x,y)\,\delta(x\cos\theta + y\sin\theta - t)\,dx\,dy; \quad -\infty < t < \infty, 0 \le \theta < \pi. \tag{1}$$

In the case of FBP technique, the Radon transform is convolved with a low pass filter $|w|$ and back-projected estimate is [15]:

$$f_{IRT}(x,y) = \int_{0}^{\pi}\int_{-\infty}^{\infty} F_{1D}\left(P_\theta(t)\right) e^{j2\pi wt}\,|w|\,dw\,d\theta. \tag{2}$$

Here, Ramachandran-Lakshiminarayan (Ram-Lak) filter has been used for simulation.

The Radon transform P_{RT} of $f_{IRT}(x,y)$ is given by:

$$P_{RT}(t,\theta) = R_a\left(f_{IRT}(x,y)\right), \tag{3}$$

where R_a is the Radon transform operator.

The discrete form representation of Sinogram P_D formed by measured projections using the data acquisition system is given by:

$$P_D(t,\theta) = \sum_{x=0}^{R_{Max}-1}\sum_{y=0}^{C_{Max}-1}\sum_{\theta=0}^{\theta_n} f(x,y)\,\zeta(\theta), \tag{4}$$

where

$$\zeta(\theta) = \begin{cases} 1 & iff \quad t = x\cos\theta + y\sin\theta \\ 0 & otherwise \end{cases}$$

Here linear interpolation has been employed to compensate for cases where the ray-sum position R_p, indicated by circles, does not coincide with the positions of detector-bins, indicated by squares, in Fig. 1. More weight of *f(x,y)* is given to the projection which is closer to R_p.

The GAs are based on the triangle of genetic reproduction, evaluation and selection [16]. The BGA cycle is shown in Fig. 2 and various implementation steps of this methodology are given below:

2.1 Initialization

The preprocessor has been fed to initialize the population *P*. The k^{th} string of *P* is given by:

$$P\left(k,(i-1)l_{side}+j\right) = f_{IRT}(i,j), \tag{5}$$

where l_{side} is the length of side of $f_{IRT}(i, j)$.

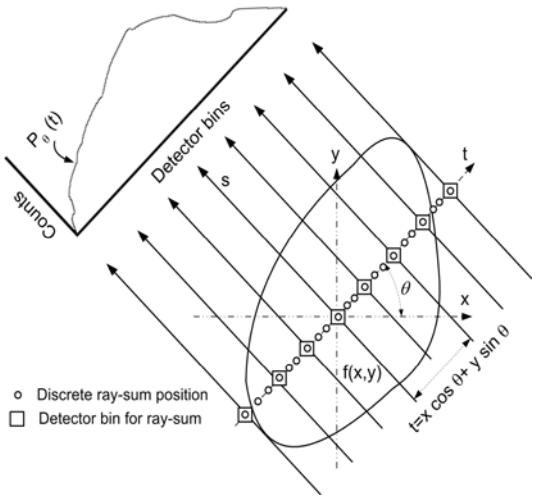

Fig. 1 Formation of a Projection at a distance t, from the centre through the object *f(x,y)* in rectangular coordinates *(x,y)*.

2.2 Selection

The selection operation provides a means for the chromosomes with better fitness to form the mating pool (MP). A mixed selection scheme has been used consisting of truncation scheme (TS) [17] followed by roulette wheel scheme (RWS) [16, 18, 19] with elitism. The details may be seen in [20].

2.3 Crossover

Conventional crossover (CO) schemes involve exchanging genes to share valuable information between each pair of mating parents. It is generally applied with high value of probability P_c. Image-row [12] and Block crossover [9] schemes have been used for this simulation as global optimizers. The region of disturbance in the former CO operator is limited to the end of the image row where as in the later case the region of disturbance consists of diagonally located rectangles in parents.

2.4 Mutation

Mutation operator allows changing slightly or completely the allele so that the resulting small variation in fitness induces diversity in the population [21]. Binary mutation operator has been used for this simulation. A random number R_{No} is generated in the range [0, 1]. The gene-bit value is flipped and assigned to the chromosome when R_{No} is less than mutation probability P_m. The algorithm for binary mutation is:

$$\text{if } R_{No} < P_m \quad N_p(i,j) = \text{flip the bit value}; \quad j = 1,2,...,n,\ i = 1,2,...,m, \tag{6}$$

where n is the total number of genes in a string and m is the total number of chromosomes.

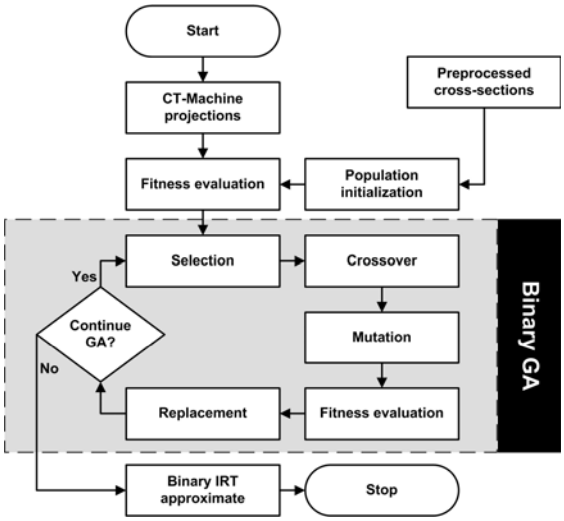

Fig. 2 Evolution cycle employed in BGA.

2.5 Fitness evaluation

The fitness function **F** chosen for maximization is based on the error between the computed and measured projections for θ_n views and t_b projections as follows:

$$\mathbf{F} = \left(1 + E_M\right)^{-1}. \tag{7}$$

Various error measures E_M that have been used are Root Mean Squared error (RMSE) [22], Mean Squared error (MSE) [23], Mean Absolute error (MAE) [24], Relative Squared error (RSE) [25], Root Relative Squared error (RRSE) [26] and Relative Absolute error (RAE) [27]. E_M for RMSE is given by:

$$E_m = \sqrt{\frac{1}{\theta_n t_b}\sum_{i=0}^{\theta_n}\sum_{j=0}^{t_b}\left\{P_{RT}(j,i) - P_D(j,i)\right\}^2}. \tag{8}$$

The termination of binary GA is carried out when a fixed number of generations have surpassed or predefined convergence level is achieved.

3. Results and Discussion

Six fitness functions have been critically evaluated for binary image reconstruction using BGA. Same set of parameters have been employed as found suitable in [20]. Binary mutation has been used with $P_m = n^{-1}$ where n represents the length of chromosome. The simulation has been based on the average of 10 repetitions for 8 × 8 phantom and 5 repetitions for 64 × 64 size. The results are shown in Table 1 and 2 for head and lung phantoms respectively. Block CO operator has been found relatively more effective than Image-row CO operator for BGA. Image quality has been measured by means of peak signal to noise ratio (PSNR) and Euclidean error (EE_{im}) of the reconstructed image [28]. Table 1 shows the minimum number of generations as 32 with MSE and 27 with MAE for 8 × 8 head and lung phantoms respectively. The reconstructed images have indeterminate PSNR and EE_{im} = 0 with best-fit individual fitness $\mathbf{F_B}$ = 1 showing that they exactly match the original phantoms. RMSE marginally outperforms RSE for 8 × 8 head phantom as shown in Fig. 3(a) but lie in the same σ-range.

Table 1. Number of generations to achieve convergence for 8 × 8 head and lung phantoms using BGA for various fitness functions with $\mathbf{F_B}$ = 1, PSNR = ∞ and EE_{im} = 0.

E_M	Ref.	Phantom	Generations
RMSE	[12]	Head	55
		Lung	57
	[9]	Head	55
		Lung	55
MSE	[12]	Head	57
		Lung	60
	[9]	Head	32
		Lung	30
MAE	[12]	Head	49
		Lung	52
	[9]	Head	41
		Lung	27
RSE	[12]	Head	50
		Lung	37
	[9]	Head	44
		Lung	43
RRSE	[12]	Head	80
		Lung	85
	[9]	Head	45
		Lung	44
RAE	[12]	Head	40
		Lung	49
	[9]	Head	35
		Lung	34

Typically, generations G = 5000 have been used for 64 × 64 image size as shown in Table 2. RMSE, MSE and RSE behave in a replicate manner as 8 × 8 phantoms.

Table 2. Image quality and $\mathbf{F_B}$ for 64 × 64 head (H) and lung (L) phantoms (P.) for reconstruction with various fitness functions using BGA.

E_M	Ref.	P.	F_B	Image quality	
				PSNR	*EE_{im}*
RMSE	[12]	H	0.7498 ± 0.0070	18.52 ± 0.47	0.5759 ± 0.0307
		L	0.9039 ± 0.055	∞	0.9007 ± 0.5234
	[9]	H	0.7671 ± 0.0144	19.26 ± 0.65	0.5295 ± 0.0407
		L	0.8837 ± 0.0216	27.20 ± 1.97	1.0772 ± 0.2281
MSE	[12]	H	0.9048 ± 0.0111	18.47 ± 0.50	0.5797 ± 0.0332
		L	0.9851 ± 0.0031	27.29 ± 1.01	1.0509 ± 0.1219
	[9]	H	0.9106 ± 0.0087	18.77 ± 0.43	0.5598 ± 0.0278
		L	0.9875 ± 0.0047	28.35 ± 1.78	0.9412 ± 0.1937
MAE	[12]	H	0.8085 ± 0.0091	15.78 ± 0.20	0.7893 ± 0.0185
		L	0.9743 ± 0.0050	28.19 ± 1.24	0.9500 ± 0.1297
	[9]	H	0.8247 ± 0.0166	16.49 ± 0.98	0.7309 ± 0.0804
		L	0.9795 ± 0.0072	29.65 ± 2.08	0.8143 ± 0.1726
RSE	[12]	H	0.9817 ± 0.0020	18.87 ± 0.45	0.5535 ± 0.0288
		L	0.7890 ± 0.0207	27.34 ± 0.56	1.0413 ± 0.0641
	[9]	H	0.9833 ± 0.0020	19.04 ± 0.53	0.5428 ± 0.0339
		L	0.8155 ± 0.0397	28.19 ± 1.24	0.9500 ± 0.1297
RRSE	[12]	H	0.8738 ± 0.0099	18.07 ± 0.94	0.6085 ± 0.0655
		L	0.6566 ± 0.0381	27.30 ± 1.64	1.0578 ± 0.1798
	[9]	H	0.8812 ± 0.0088	18.42 ± 0.53	0.5826 ± 0.0346
		L	0.7016 ± 0.0473	29.04 ± 2.34	0.8770 ± 0.2010
RAE	[12]	H	0.8763 ± 0.0084	15.59 ± 0.56	0.8075 ± 0.0529
		L	0.8379 ± 0.0719	28.79 ± 2.98	0.9197 ± 0.2958
	[9]	H	0.8989 ± 0.0058	16.93 ± 0.78	0.6935 ± 0.0634
		L	0.7996 ± 0.0259	26.95 ± 0.92	1.0918 ± 0.1119

For 8 × 8 lung phantom, MSE and MAE attained convergence using relatively lesser G whereas for 64 × 64 lung phantom MSE, MAE and RRSE achieved similar image quality although the $\mathbf{F_B}$ for RRSE was low.

Rapid changes in convergence trends have been observed in Fig. 3(a), (b) and 4(a), (b) for 8 × 8 head and lung phantoms respectively. This is attributed to the fact that, near convergence, only one good gene-flipping may fully converge it.

The starting point for each plot for $\mathbf{F_B}$ and PSNR is different depending on the preprocessor used for population initialization. A fall in PSNR during initial generations is attributed to the higher probability of improvement in $\mathbf{F_B}$.

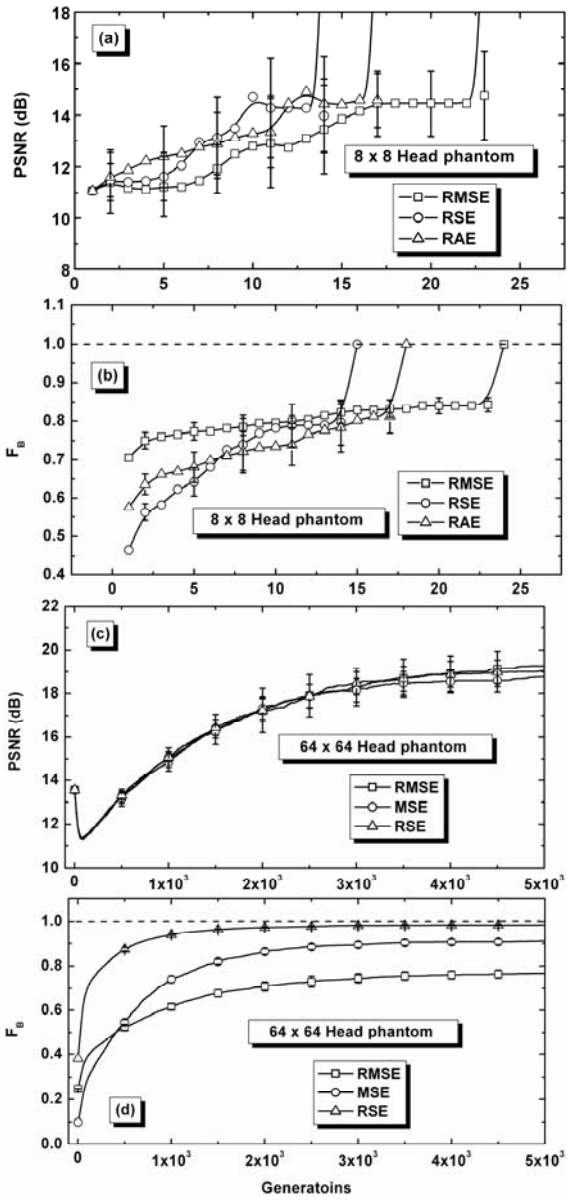

Fig. 3 Convergence trend for reconstructed head phantom using BGA, (a) & (c) variation of PSNR and (b) & (d) showing variation of FB for 8 × 8 & 64 × 64 phantoms.

4. Conclusions

The Binary Genetic Algorithm (BGA) based fitness function evaluation has been carried out for parallel-ray transmission tomography employing FBP based population initialization.

- The various fitness functions studied include Root Mean Squared error (RMSE), Mean Squared error (MSE), Mean Absolute error (MAE), Relative

Squared error (RSE), Root Relative Squared error (RRSE) and Relative Absolute error (RAE).

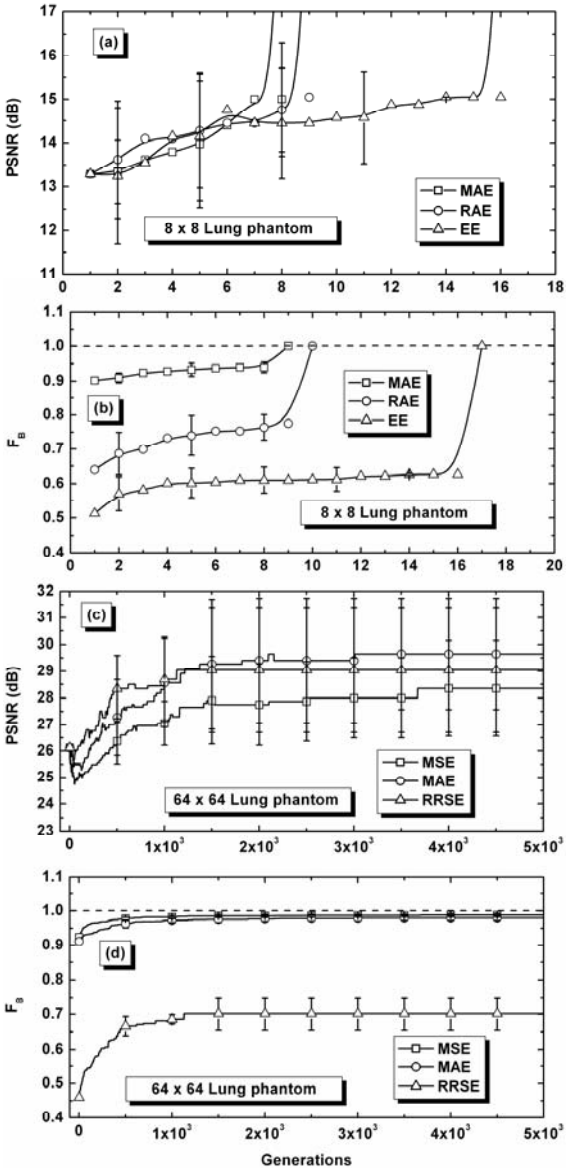

Fig. 4 Convergence trend for reconstructed lung phantom using BGA, (a) & (c) variation of PSNR and (b) & (d) variation of $\mathbf{F_B}$ for 8 × 8 & 64 × 64 phantoms.

- RMSE and MAE have been found superior compared with the remaining fitness functions as far as better convergence and higher sensitivity are concerned.
- Block crossover operator coupled with binary mutation operation for 64 × 64 head phantom and lung phantom has resulted in PSNR values with RMSE 19.26 & 16.49 respectively and 27.20 & 29.65 dB with MAE.

Acknowledgments

S. A. Qureshi acknowledges funding by Higher Education Commission, Pakistan under PIN No. 041 103076 Cu-027.

References

[1] S. A. Qureshi and S. M. Mirza, "Inverse Radon transform-based image reconstruction modalities," in National Conference on Information Technology and Applications, 13-25, 2005.

[2] D.-S. Luo and A. E. Yagle, "A Kalman filtering approach to stochastic tomography," in IEEE International Conference on Acoustics, Speech, and Signal Processing, 2589-2592, 1991.

[3] N. Metroplis, A. W. Rosenbluth, A. H. Teller and E. Teller, "Equations of state calculations by fast computing machines," Journal of Chemical Physics. 21, 1087-1092, 1953.

[4] M. W. Trosset, "What is simulated annealing?" Optimization and Engineering. 2, 201-213, 2001.

[5] W. H. Press, S. A. Teukolsky, W. T. Vetterling and B. P. Flannery, Numerical recipes in C: The art of scientific computing, Cambridge University Press, New York, 2002.

[6] S. A. Qureshi, S. M. Mirza and M. Arif, "Hybrid Simulated Annealing Image Reconstruction for Parallel-Ray Transmission Tomography," Journal of Mathematical Imaging and Vision, in Process, 2005.

[7] J. H. Holland, "Outline for logical theory of adaptive systems," J. ACM. 3, 297-314, 1962.

[8] J. H. Holland, Adaptation in natural and artificial systems, University of Michigan Press, Ann Arbor, MI, 1975.

[9] L. Franconi and C. Jennison, "Comparison of a genetic algorithm and simulated annealing in an application to statistical image reconstruction," Statistics and Computing. 7, 193-207, 1997.

[10] X. Li, T. Jiang and D. J. Evans, "Medical Image Reconstruction Using a Multi-objective Genetic Local Search Algorithm," International Journal on Computer Mathematics. 74, 301-314, 2000.

[11] T. Günel and S. Kent, "Genetic approach for the determination of object parameters from x ray projections," Electrik. 6, 277-286, 1996.

[12] S. A. Qureshi, S. M. Mirza and M. Arif, "A Hybrid Continuous Genetic Algorithm for Parallel-ray Transmission Tomography Image Reconstruction," Imaging Science Journal, The, in Process, 2006.

[13] L. A. Shepp and B. F. Logan, "The Fourier reconstruction of a head section," IEEE Trans. Nucl. Sci. NS-21, 21-43, 1974.

[14] A. K. Jain, Fundamentals of Digital Image Processing, Pearson Education, Singapore, 1989.
[15] A. C. Kak and M. Slaney, Principles of Computerized Tomographic Imaging, IEEE Press, New York, 1988.
[16] D. E. Goldberg, Genetic algorithms in search, optimization and machine learning, Addison-Wesley, Reading Massachusetts, 1989.
[17] T. Back, F. Hoffmeister and H. P. Schwefel, "A Survey of Evolution Strategies," in Fourth International Conference on Genetic Algorithms, 2-9, 1991.
[18] J. Koza, Genetic programming: On the programming of computers by means of natural selection. MIT press, Cambridge, Massachusetts, 1992.
[19] M. Mitchell, An introduction to genetic algorithms, MIT Press, Cambridge, Massachusetts, 1999.
[20] S. A. Qureshi, S. M. Mirza and M. Arif, "Determination of Optimal Number of Projections for Parallel-Ray Transmission Tomography using Hybrid Continuous Genetic Algorithm," International Journal of Imaging Systems and Technology, in Process, 2006.
[21] M. Bessaou and P. Siarry, "A genetic algorithm with real-value coding to optimize multimodal continuous functions," Struct Multidisc Optim. 23, 63-74, 2001.
[22] J. O. Smith, Mathematics of the Discrete Fourier Transform (DFT), W3K Publishing, Stanford, California, 2002.
[23] H. P. Hsu, Theory and Problems of Probability, Random Variables, and Random Processes, McGraw-Hill, New York, 1997.
[24] T. M. Le, W. M. Snelgrove and S. Panchanathan, "Fast Motion Estimation Using Feature Extraction and XOR Operations," in SPIE Proceedings of Multimedia Hardware Architectures, 108-118, 1998.
[25] B. Arnold, "Some properties of the relative squared error approach to linear regression analysis," Statistics. 38, 183-193, 2004.
[26] X. Inters, V. Ntziachrostos, J. Culver, A. Yodh and B. Chance, "Projection access order in algebraic reconstruction technique for diffuse optical tomography," Physics in Medicine and Biology. 47, N1-N10, 2001.
[27] E. Kreyszig, Advanced Engineering Mathematics, John Wiley & Sons, New York, 1993.
[28] S. A. Qureshi, S. M. Mirza and M. Arif, "Quality of inverse radon transform based image reconstruction using various algorithms in transmission tomography," Science International. 18(3), 181-186, 2006.

S. A. Qureshi is a Ph.D. candidate at the Department of Computer and Information Sciences, PIEAS, Pakistan. His main interests are the filtered & transform-based image processing techniques, Wavelet transforms, Genetic algo-rithms, Simulated Annealing and Neural Networks.

Sikander M. Mirza is a Professor in the Department of Physics & Applied Mathematics and member of the Computational Physics Group at the PIEAS. He is also member of the Computational Intelligence Group of the Department of Computer & Information Science at PIEAS. He has served as Head of the Physics & Applied Mathematics Department (2001-2006), and currently serving as Dean of Faculty of Applied Sciences at PIEAS with main research interest in Computational Physics, Modeling & Simulation and Advanced Numerical Techniques. He has published numerous papers in several areas including Numerical Methods, Computational & Simulation Physics and Applied Physics.

M. Arif is an Associate Professor in the Department of Electrical Engineering at the PIEAS, Pakistan. He has served as Head of the Electrical Engineering Department. His main research interests are Signal processing, Data fusion, Image processing and Machine vision.